Neoplasia • Vol. 9, No. 12, December 2007, pp. 1130–1137

www.neoplasia.com

# Tracking the Migration of Dendritic Cells By *In Vivo* Optical Imaging[1]

*Wellington Pham, Jingping Xie and John C. Gore*

Vanderbilt University Institute of Imaging Science, 1161 21st Ave. S., AA-1105 MCN, Nashville, TN 37232-2310, USA

**Abstract**

**We report herein a method to track the migration of dendritic cells (DCs) using optical imaging. With the assistance of the delivery module, fluorescein isothiocyanate (FITC) could internalize inside DCs within 15 minutes of incubation. The fluorescent signal was mostly cytoplasmic and could be detected using *in vivo* imaging. Furthermore, we observed that the probe did not interfere with the DCs maturation as we assessed the expression of several surface markers. The labeled DCs secreted interleukin-12 (IL-12) and tumor necrosis factor–alpha (TNF-$\alpha$) and stimulated the proliferation of $CD4^+$ T lymphocytes responding to lipopolysaccharide (LPS) stimulation. We have systematically compared the probe uptake between mature and immature DCs. The study showed that the latter phagocytosed the probe slightly better than the former. Intravital imaging of treated mice showed the migration of DCs to lymph nodes (LNs), which is confirmed by immunohistochemistry. Taken together, we demonstrated the potential use of optical imaging for tracking the migration of DCs and homing *in vivo*. The delivery molecules could also be used on other imaging modalities or for delivery of antigens.**

*Neoplasia* (2007) **9,** 1130–1137

**Keywords:** Dendritic cells, optical imaging, delivery, lymph node, antigen-presenting cells.

## Introduction

Dendritic cells (DCs) play an important role in the initiation and development of adaptive immune responses against bacteria, viruses, allergens, and tumor antigens [1]. They are the most effective antigen-presenting cells because they can capture and take up antigens in the peripheral tissues and transport these antigens from the peripheral sites to the primary and secondary lymphoid tissues for T-cell presentation [2]. The functional characteristics of DCs evolve with their stage of maturation [3]. Immature DCs have no ability to activate T lymphocytes, but they are strategically located at body surfaces and in interstitial spaces of most tissues [4]. The primary function of this stage of cellular development is to capture microbial protein antigens through their active phagocytosis mechanisms. During the migration to lymphoid tissues, DCs undergo further differentiation that can be characterized by the loss of phagocytotic capacity and increased expression of costimulatory surface molecules necessary for T-cell activation through the major histocompatibility–peptide complexes. Recently, several lines of research have demonstrated the successful use of DCs for generating antitumor immune responses in animals. In these studies, DCs were pulsed with tumor-associated antigen peptide or protein to elicit antigen-specific protective antitumor immunity in a number of murine models [5,6]. This observation laid the foundation for several clinical studies using the same approach [7–12]. The clinical works showed promise, but the results have been mixed, mainly because the progress in this area has been severely limited by the lack of effective methods for monitoring the behavior of DCs *in vivo*, both in animals, and more crucially, in human following reinjection of activated DCs into the host system [13,14]. Another hurdle in this field is that the majority of the work depends on histological staining that requires the sacrifice of the animals to determine the mobility and interaction of DCs with other cells at the target sites [15], thus limiting the ability to obtain information regarding the dynamic cell migration, homing, and, importantly, cellular fate in a living system. To achieve optimal and translational research parallel to and eventually valuable to clinical applications, we decided to use optical imaging as a means to track the migration of DCs *in vivo*.

In this work, we describe a method to deliver a fluorescent dye using a myristoylated polyarginine (11-mer) peptide ($MPA_{11}P$) module. The presence of a fluorescent dye enables us to quantify the uptake at different stages of the development of DCs. Most importantly, we can track cell migration to the peripheral lymphatic tissue using the whole mouse optical imaging system and the data are corroborated with immunohistochemistry.

Abbreviations: BrdU, bromodeoxyuridine; DC, dendritic cell; DIC, differential interference contrast; FCS, fetal calf serum; FITC, fluorescein isothiocyanate; LN, lymph node; $MPA_{11}P$, myristoylated polyarginine (11-mer) peptide

Address all correspondence to: Wellington Pham, Vanderbilt University Institute of Imaging Science, 1161 21st Ave. S., AA-1105 MCN, Nashville, TN 37232-2310, USA. E-mail: wellington.pham@vanderbilt.edu

[1]The National Institute on Aging grant AG026366-01A1 and the Vanderbilt University School of Medicine Department of Radiology start-up fund provided support for this work. Finally, animal work was supported by the Small Animal Imaging Resource Program grant U24 CA126588.

Received 21 September 2007; Revised 8 October 2007; Accepted 9 October 2007.



DOI 10.1593/neo.07586

## Materials and Methods

Adult C57BL/6 (H-2b) mice were obtained from The Jackson Laboratory (Bar Harbor, ME). Animal experiments were carried out in accordance with the guidelines provided by Vanderbilt University Institutional Animal Care and Use Committee (IACUC) and the National Institute of Health Guide for the Care and Use of Laboratory Animals. Granulocyte/macrophage colony–stimulating factor (GM-CSF) and interleukin-4 (IL-4) came from PeproTech (Rocky Hill, NJ). Lipopolysaccharide (LPS) derived from *Escherichia coli* and fluorescein isothiocyanate (FITC) were purchased from Sigma-Aldrich (St. Louis, MO). Monoclonal antibodies against CD16/CD32, CD11c, CD80, CD86, and CCR7 as well as their biotin-labeled isotypic antibodies were purchased from eBioscience (San Diego, CA). Paired antibodies for enzyme-linked immunosorbent assay (ELISA) detection of tumor necrosis factor–alpha (TNF-$\alpha$) and IL-12 and other reagents for ELISA were also purchased from eBioscience. T4 cell isolation and bromodeoxyuridine (BrdU)-based proliferation kits were purchased from BD PharMingen (San Diego, CA). RPMI 1640, fetal calf serum (FCS), and other cell culture additives came from Invitrogen (Carlsbad, CA).

### *Dendritic Cells Preparation*

Dendritic cells were isolated from mouse bone marrow as described with slight modifications [16]. Briefly, marrow cells were flushed out from femurs and tibias of C57BL/6 mice and subsequently passed through wire mesh screens to obtain a single cell suspension. Red cells were lysed with 0.83% ammonium chloride twice with 2 minutes of incubation at room temperature each time. The remaining cells were cultured with RPMI 1640 supplemented with 10% FCS, 50 $\mu$M 2-mercaptoethanol, 100 mM sodium pyruvate, 100 U/ml penicillin, 100 $\mu$g/ml streptomycin, and 1000 U/ml recombinant GM-CSF (rGM-CSF) and IL-4. On day 3 of the culture, nonadherent granulocytes and the B and T lymphocytes were gently removed by suction of 75% of the medium and fresh media were added. The released immature, nonadherent cells were collected on day 5 with typical morphologic features of DCs. Immature DCs were used on day 6. Maturation of the DCs was achieved by culturing the cells in a similar manner. On day 7, the DCs were stimulated with 10 ng/ml TNF-$\alpha$ or 10 $\mu$g/ml LPS for 48 hours.

### *$CD4^+$ T-Cells Preparation*

A purified population of $CD4^+$ T lymphocytes was obtained from freshly harvested splenocytes by negative selection columns with a CD4 magnet-bead, according to the manufacturer's specifications (BD PharMingen). Cells purified using this method were 90% positive for selected T-cell phenotype.

### *$MPA_{11}P$-FITC Probe*

The development of the $MPA_{11}P$-FITC probe in this study was described previously [17,18]. Briefly, a myristic acid moiety was incorporated into the 11-mer polyarginine peptide through a $\beta$-alanine spacer. The peptide also contains a lysine analog at the C-terminal for dye labeling. FITC was attached into the lysine side chain in the presence of diisopropylethylamine. The synthesized compound was purified by high-performance liquid chromatography and characterized by matrix-assisted laser desorption and ionization time-of-flight mass spectrometry; calculated: 2535.45, found: 2535.73 $(M + H)^+$.

### *Labeling Dendritic Cells*

The $MPA_{11}P$-FITC probe was diluted at the indicated concentrations with Hank's balanced salt solution. Two milliliters of the probe was used in each 60-mm dish seeded with $0.5 \times 10^6$ cells. After incubating at 37°C in a humidified atmosphere with 5% $CO_2$ for either 15 or 60 minutes, the excess probe was washed three times with phenol red–free Hank's balanced salt solution. The labeled cells were either maintained in full-growth media for future experiments or directly collected for fluorescence-activated cell sorting (FACS) analysis to assess the labeling efficiency. FITC alone was used as a reference control while quantifying the probe uptake in both immature and mature DCs. When assessing the effect of probe labeling on the function of DCs, such as surface marker expression and cytokine secretions, the controls were the untreated immature DCs.

### *Fluorescence Microscopy on Live Cells*

Mature or immature DCs ($2.0 \times 10^4$) were plated in separate wells of an eight-well chamber (Nalge Nunc International, Rochester, NY) in full-growth medium overnight. The cells were then labeled with either 0.2 $\mu$M of FITC (control) or $MPA_{11}P$-FITC for 15 minutes at 37°C in a 5% $CO_2$–equipped incubator. Cells were washed three times with PBS and directly examined under a fluorescence microscope with the cells covered by a thin layer of PBS. Confocal microscopy of the unfixed cells was performed using an inverted microscope (LSM510; Zeiss, Thornwood, NY). Images were acquired with 488-nm excitation and 515-nm emission for both control FITC and $MPA_{11}P$-FITC. Transmitted light differential interference contrast (DIC) images were also acquired.

### *Enzyme-Linked Immunosorbent Assay*

Enzyme-linked immunosorbent assay was used to quantify the secreted IL-12 and TNF-$\alpha$ during the DCs' maturation. Briefly, a 96-well plate (Corning, Lowell, MA) was coated with 0.2 $\mu$g of purified anti–IL-12 or anti–TNF-$\alpha$ antibody (eBiosciences) in 100 $\mu$l of PBS overnight at 4°C, washed twice with PBS–T (0.05% Tween-20 in PBS), and nonspecific binding blocked for 3 hours at room temperature with 5% BSA in PBS. The plates were washed and aliquots (10, 50, and 100 $\mu$l) of centrifuged culture medium were added into the plate (the volume was made up to 100 $\mu$l with fresh culture medium). The plates were then incubated for 2 hours at room temperature, followed by six washes with PBS–T. Purified and biotinated conjugated monoclonal antibodies (100 $\mu$l of 1 $\mu$g) against IL-1 and TNF-$\alpha$ in PBS–T and 1% BSA were added to corresponding wells in the plates for 2 hours of incubation at room temperature. The plate was washed and incubated

with 100 μl of 1:500 (with PBS–T/1% BSA) diluted HRP–avidin (eBiosicence) for 30 minutes at room temperature. After washing (four times) with PBS–T and with PBS (twice), colorimetric detection at 492 nm on the plate reader was performed using *O*-phenylenediamine dihydrochloride as substrate (Sigma FAST OPD tablet). Each sample was measured in three different dilutions. Data were presented as the average of a triplicate with standard deviation.

*Phantom and* In Vivo *Optical Imaging*

Optical imaging experiments were carried out on female mice, 7 to 8 weeks of age. To enhance the detection in an *in vivo* study, we briefly incubated mature DCs with freshly developed probe (6 μM). Two million labeled DCs were adaptively transferred to C57BL/6 mice through subcutaneous (s.c.) injection. Right after injection, animals were anesthetized with isoflurane and imaged as an initial point. Twenty-four–hour postinjection, the same process was repeated. Then the lymph nodes (LNs) were exposed and imaged. Phantom and *in vivo* imaging were performed using a fluorescence reflectance whole-mouse system (IVIS 200; Xenogen, Cranbury, NJ). Images were acquired using the IVIS imaging system with the excitation at 490 nm and the fluorescence was collected through a long-pass filter. Data were analyzed by Living Image software version 2.5 (Cranbury, NJ).

*Cell Surface Phenotyping*

Surface antigens were analyzed on day 7 or 9 of the culture following maturation by flow cytometry. Dendritic cells were preincubated with anti–CD16/32 to block nonspecific Fc interaction for 10 minutes. Aliquoted cells were then incubated with biotinylated monoclonal antibodies specific for selective surface markers of DC maturation (CD11c, CD80, CD86, and CCR7) for 20 minutes at 4°C, washed twice with PBS, and developed with streptavidin–phycoerythrin. The control group was incubated with biotinylated isotypic immunoglobins and was also developed with streptavidin–phycoerythrin. Flow cytometric analysis was performed using a FACSCalibur (BD Biosciences, Mountain View, CA) with CellQuest software (BD Biosciences). Gating was performed according to light scattering properties, and dead cells were excluded based on their forward/side scatter pathway.

*Mixed Leukocyte Reactivity Assay*

The ability of DCs to stimulate quiescent T-cells was assessed by the mixed leukocyte reactivity assay. Unstimulated or LPS-stimulated DCs with or without labeling with $MPA_{11}P$-FITC were harvested, washed, and irradiated at a dose of 30 Gy and plated at serial dilutions in 24-well plates. These stimulator DCs were incubated for 3 days with 100×, 20×, and 5× (T-cell/DC ratio) splenic $CD4^+$ T-cells in RPMI 1640 media supplemented with 10% heat-inactivated FCS, 2 mM glutamine, 100 U/ml penicillin, streptomycin, and nonessential amino acids, and 1 mM sodium pyruvate, and were then incubated at 37°C under 5% $CO_2$ atmosphere for 3 days. BrdU was added for the last 24 hours. BrdU integration–based proliferation assay was performed with a kit, using the procedure recommended by BD Bioscience.

*Immunohistological Procedures*

After completion of the *in vivo* imaging experiment, animals were sacrificed and the inguinal LNs were excised and snap frozen in liquid nitrogen. Five-micrometer sections of frozen LN tissues were placed on charged slides. The samples were treated with Ultra V block for 5 minutes (Labvision, Fremont, CA) for nonspecific staining before primary antibody addition. Tissues were incubated with goat anti-CD3 (cat. # SC-1127; Santa Cruz Biotechnology, Inc., Santa Cruz, CA) diluted 1:200 for 60 minutes followed by donkey anti–goat Rhodamine (Invitrogen) at 1:500 for 30 minutes. Microscopy was performed using a confocal microscope (LSM 510Meta; Zeiss) equipped with an LSM Pascal Vario RGB Laser Module (argon/2 458, 477, 488, and 514 nm; HeNe1 543 nm; and HeNe2 633 nm; Thornwood, NY). Images with slice thickness of < 0.9 μm were acquired to produce FITC and Rhodamine staining. Summation projection of all background-corrected confocal slices was produced using the LSM Pascal Software (v. 3.2 WS). Final confocal images were color-coded green for FITC and red for Rhodamine.

*Statistical Analysis*

Data were expressed as means ± SD. Statistical differences were performed using Student's *t* test (GraphPad software, San Diego, CA). Significance was considered for $P < .05$.

## Results

The current challenge we face in tracking DCs *in vivo* is that most imaging probes have low permeability for DCs. Although described as antigen-presenting cells, DCs display poor endocytic and phagocytic capacities [19,20]. Therefore, we theorized that successful tracking of labeled DCs by imaging would need a robust and expeditious delivery of the probe inside the cells. In the present study, we test our theory by using the previously described and reported novel class of membrane translocation peptides to shuttle the fluorescent dye inside the DCs, followed by an injection of the labeled DCs into syngeneic mice for tracking the migration of the labeled cells using optical imaging. The amphiphilic delivery module was composed of a myristic acid linked to 11-mer polyarginine peptide ($MPA_{11}P$) through a β-alanine linker, whereas the fluorescent dye, FITC, was attached to the delivery module through a lysine side chain [17].

We tested cell uptake by FACS analysis using two different concentrations. There was minimal internalization of FITC at a concentration of 0.2 μM in both mature and immature DCs, even after 1 hour of incubation (Figure 1).

There was an insignificant fluorescent signal enhancement when the FITC concentration increased to 1.0 μM. However, we did not anticipate that the optical imaging device could detect this diminutive internalized signal. This is a fundamental difference between *in vivo* optical imaging

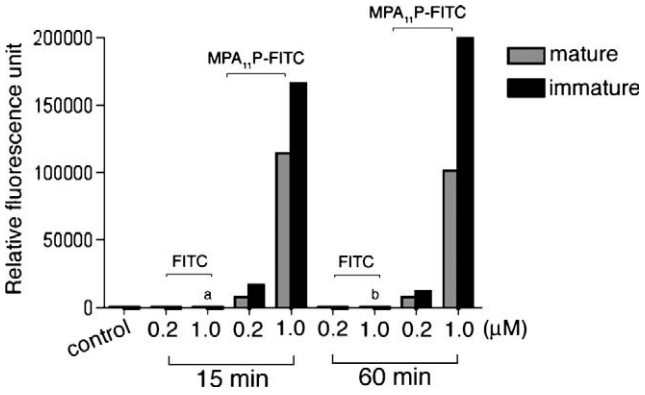


**Figure 1.** *Mature versus immature DCs on the ability to uptake the probe. Half of the isolated DCs was incubated with FITC or the $MAP_{11}$P-FITC probe at two different concentrations and times. Cell-associated materials were quantified by FACS analysis. The other half of the population was allowed to mature for 2 days, followed by a similar study.* [a] *The fluorescent signals were 2- and 4-fold compared to the control for mature and immature DCs, respectively.* [b] *The signal was 3-fold compared to the control for both mature and immature DCs. The results shown represent the mean of two independent experiments.*

and *in vitro* fluorescence microscopy. The latter has been used mostly for imaging frozen sections for carboxylfluorescein succinimidyl ester–labeled DCs [21]. By contrast, when FITC was attached to $MPA_{11}$P to form an $MPA_{11}$P-FITC probe with a final concentration of 0.2 μM, both mature and immature DCs showed remarkable uptakes. When the concentration of the probe was increased to 1.0 μM, the uptakes were very significant. To our surprise, we found that there was no further improvement for lengthening incubation time beyond 15 minutes in either mature or immature DCs. These results suggest that the delivery-assisted transport of FITC into DCs was very efficient and could be achieved in a notably short period of time.

FACS provides quantitative values, but it does not give an overall picture of cellular distribution. In the next assay, we examined the dynamic localization of the probe in mature and immature DCs using confocal microscopy. Figure 2 shows that the morphology of immature and mature DCs can be distinguished readily using the differential integration contrast (DIC) channel. The former have a round shape whereas the latter have a dendrite-like features on the cell surface. A 15-minute incubation of $MPA_{11}$P-FITC (0.2 μM) resulted in remarkable fluorescent signals in both mature and immature DCs. However, neither showed any degree of uptake for an equivalent concentration of FITC (Figure 2*A*). Furthermore, confocal microscopic data showed that the delivery module carried the fluorescent dye across the cell membrane and homing to the cytoplasm. We also observed that immature DCs phagocytosed the probe slightly more effectively than do their mature counterparts. Quantitative

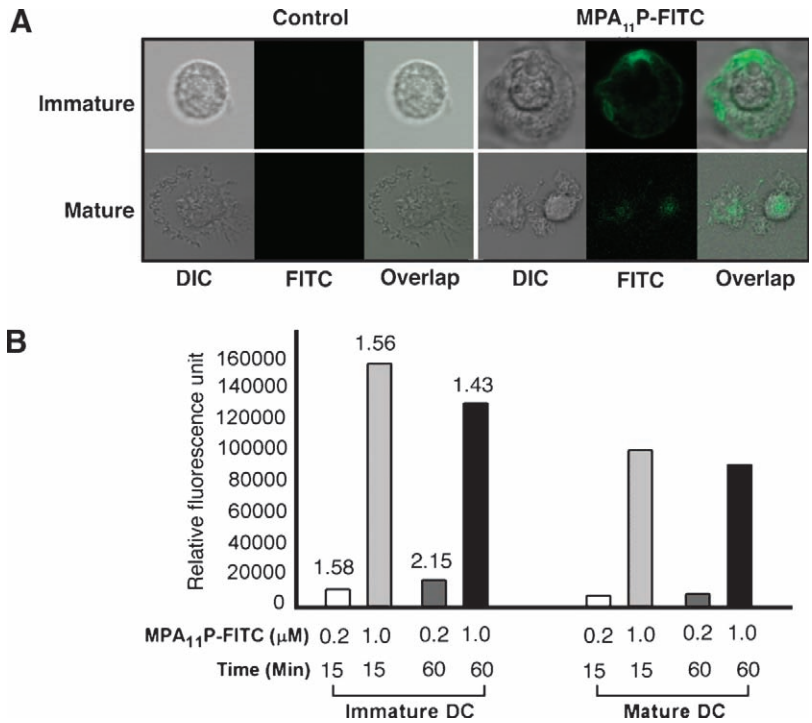


**Figure 2.** *Comparison of the uptake of DCs at different stages of cellular development. (A) Confocal microscopy on live cells plated on the eight-well Nalge Nunc chambers on incubation with either 0.2 μM of a fluorescent dye of FITC or with probe $MPA_{11}$P-FITC for 15 minutes at 37°C. The morphologies of mature and immature cells are distinguished on the DIC channel. Images were color-coded green for FITC. Fluorescence images indicate that the delivery module shuttles the dye inside DCs with remarkable efficiency. The signal is perinuclear and mostly cytosolic. To generate a better localization, the fluorescence image was merged with DIC. (B) Immature DCs uptake better than mature counterparts. Bone marrow–derived DCs were isolated; on day 6, half of the cells were treated with the probe at the indicated time and the uptake was quantified by FACS analysis. LPS was added to the rest of the cells and they were allowed to grow over a period of 2 days. The mature cells were then treated in a similar manner as described for the immature counterparts. The uptake of immature DCs was, to some extent, better at every tested concentration. The results shown represent the mean of two independent experiments.*

FACS analysis showed that it is about 1.5- to 2-fold better (Figure 2*B*).

Continuing work showed that the $MPA_{11}$P-FITC probe not only crossed inside DCs effectively, but that it was also nontoxic. As a consequence, there were no observed adverse effects on cellular functionality. Figure 3*A* shows that the phenotypes of the labeled and the unlabeled control cells appear to be similar on the upregulation of the maturation process (CD11c), expression of the costimulatory surface molecules (CD80 and CD86), and the cytokine receptor (CCR7). Functional assays were carried out to analyze the levels of the secreted IL-12 and TNF-$\alpha$ from activated labeled and unlabeled DCs compared to nonactivated controls. ELISA analysis of the cell supernatant revealed that IL-12 and TNF-$\alpha$ were about 39- and 19-fold higher, respectively, in the labeled cells compared to nonactivated cells. For comparison, under identical conditions, secretion of IL-12 and TNF-$\alpha$ of unlabeled cells increased about 45- and 21-fold, respectively, after LPS-induced activation (Figure 3*B*). These data suggest that labeling DCs with the $MPA_{11}$P-FITC probe might decrease the secretion of cytokines slightly, compared to the unlabeled cells.

Next, we investigated the ability of labeled DCs to induce T-cell proliferation. Dendritic cells were incubated with the probe before LPS-induced maturation or were freshly labeled after LPS treatment. With corresponding controls, all DCs were irradiated to halt proliferation. Designated and diluted DCs were then cocultured with freshly prepared splenic $CD_4^+$ T-cells. The ability of DCs to stimulate the proliferation of $CD_4^+$ T-cells was assessed by a FACS assay based on the BrdU integrations. As shown in Figure 3*C*, coculturing with DCs compared to T-cells alone stimulates $CD_4^+$ T-cell proliferation. LPS-stimulated DCs further enhanced the proliferation of cocultured T-cells in all three tested DC populations. Both pre- and postlabeling with the probe have minimal effect on the potential of the DCs to stimulate $CD_4^+$ T-cells. Altogether, these data support the notion that labeling DCs using our $MPA_{11}$P-FITC probe does not interfere with the surface receptor expression, the phenotype, or the functions of the DCs, nor does it affect the ability to communicate with T-cells through secretory cytokine.

To demonstrate the possibility that this technique can be used for *in vivo* application, first, we performed imaging on phantom tubes. Half a million DCs were incubated with either 0.2 $\mu$M $MPA_{11}$P-FITC probe or an equal amount of FITC as a control for 15 minutes; and then, the cells were transferred to the tubes that had been precasted with 5% agarose gel.

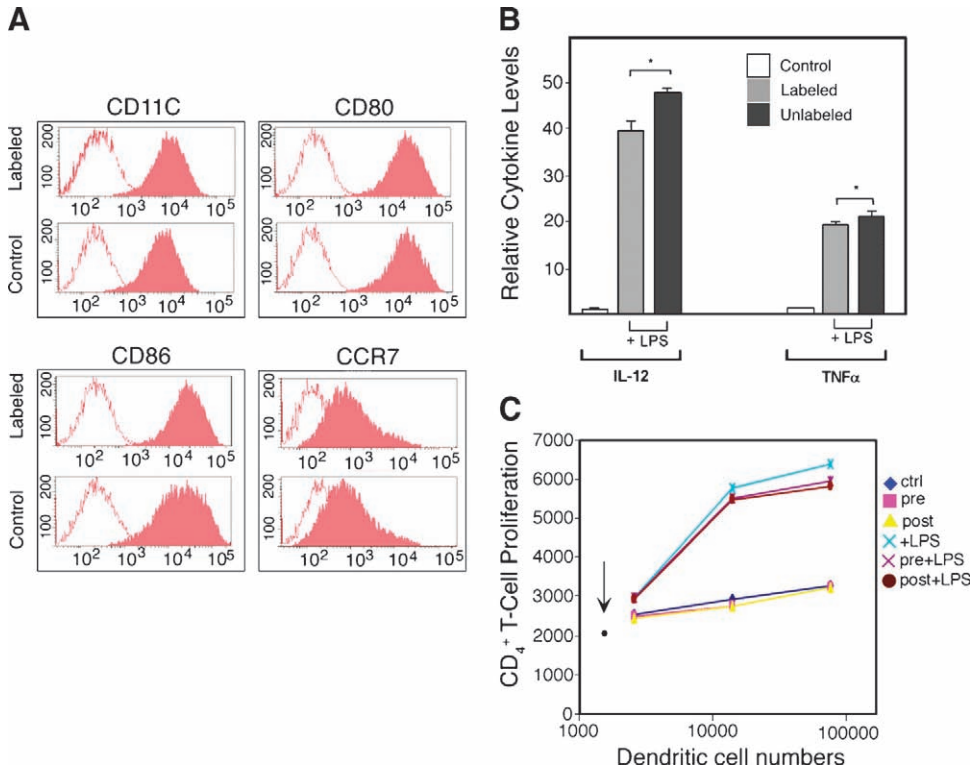


**Figure 3.** *Phenotypical and functional study of labeled DCs. (A) FACS profiles of surface markers expression of CD11c, CD80, CD86, and CCR7. The shaded histogram represents the indicated specific antibody; the open histogram is the isotype control antibody. (B) Isolated bone marrow–derived DCs were divided into three groups. The first group was treated with buffer; the second and third groups were activated with LPS, and one of them was treated with buffer as control and the other with the $MPA_{11}$P-FITC probe. Secretions of IL-12 and TNF-$\alpha$ were measured in the supernatants using ELISA. Results are shown as means ± SD of triplicate values and statistical analysis was performed using Student's t test, $P < .05$. (C) The abilities of the labeled and mature DCs to induce $CD_4^+$ T-cell proliferation were compared with the ability of the unlabeled mature DCs. In this assay, the incorporation of BrdU into the newly synthesized T-cells was stained with specific anti–BrdU fluorescent antibodies. The degree of cell-associated BrdU was then measured by FACS analysis. Labeling DCs when they were immature (Pre) or mature (Post) without activation by LPS did not induce T-cell proliferation; consequently, we observed the levels of T-cell counts to be as low as the control. In contrast, activation of DCs with LPS in either mature (LPS + Post) or immature status (Pre + LPS) stimulated $CD_4^+$ T-cell proliferation.*

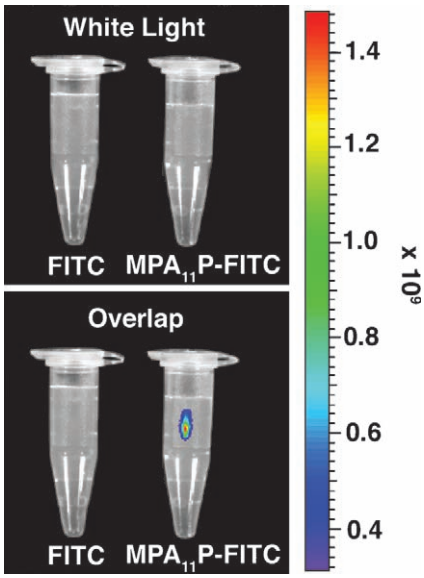


**Figure 4.** *Mature DCs were incubated with the $MPA_{11}$P-FITC probe for 15 minutes and the fluorescent signal was readily detected in phantom imaging.*

Images were obtained using the IVIS optical imaging device. The fluorescent signals of labeled cells from the phantom tubes were remarkably strong (Figure 4), whereas the FITC-labeled cells did not show any signal ($P < .0001$).

Next, we determined whether optical imaging could be used to monitor cell migration and homing *in vivo*. The labeled DCs were adaptively transferred into C57BL/6 mice ($n = 5$) by s.c. injection. The LN was surgically exposed 24 hours after injection, and the fluorescent signal was detected in the LN with a distinct intensity compared to the control muscle tissue (Figure 5). Dual-channel fluorescence microscopy of the dissected LN showed a strong signal, and this corroborated the *in vivo* imaging data. Notably, the fluorescent signal merged with CD3-specific T-cell markers, indicating that DCs inside the LN preferentially accumulated in the T-cell area (paracortex).

## Discussion

The hypothesis that tumor antigen–bearing DCs could be used as a vaccine to prevent tumors or to kill existing tumors forms the underlying basis for many clinical trials designed to test the possibility of using DCs to induce immunity against antigens associated with many tumors including breast, lung, prostate, and melanoma [22]. However, many issues need to be resolved in basic research; one of the priorities is to examine cellular functionality after the *in vitro* stimulation with tumor antigens, as well as the mobility and cellular fate after adaptive transferred of the cells in the host system. *In vivo* detection of the migration of DCs would be an important tool for further research of the role DCs play in developing effective cancer vaccines. In this work, we demonstrate that it is feasible to track the migration of DCs *in vivo* using a whole-mouse optical imaging system. Several experiments carried out in our laboratory indicated that DCs cannot appreciably uptake imaging probes (data not shown). Therefore, we propose to use a delivery-assisted strategy to address this problem. With the assistance of the delivery module, FITC can be shuttled inside DCs sufficiently in both mature and immature cells, and in a remarkably short period of time (15 minutes). Other researchers have shown that the average uptake time of materials by

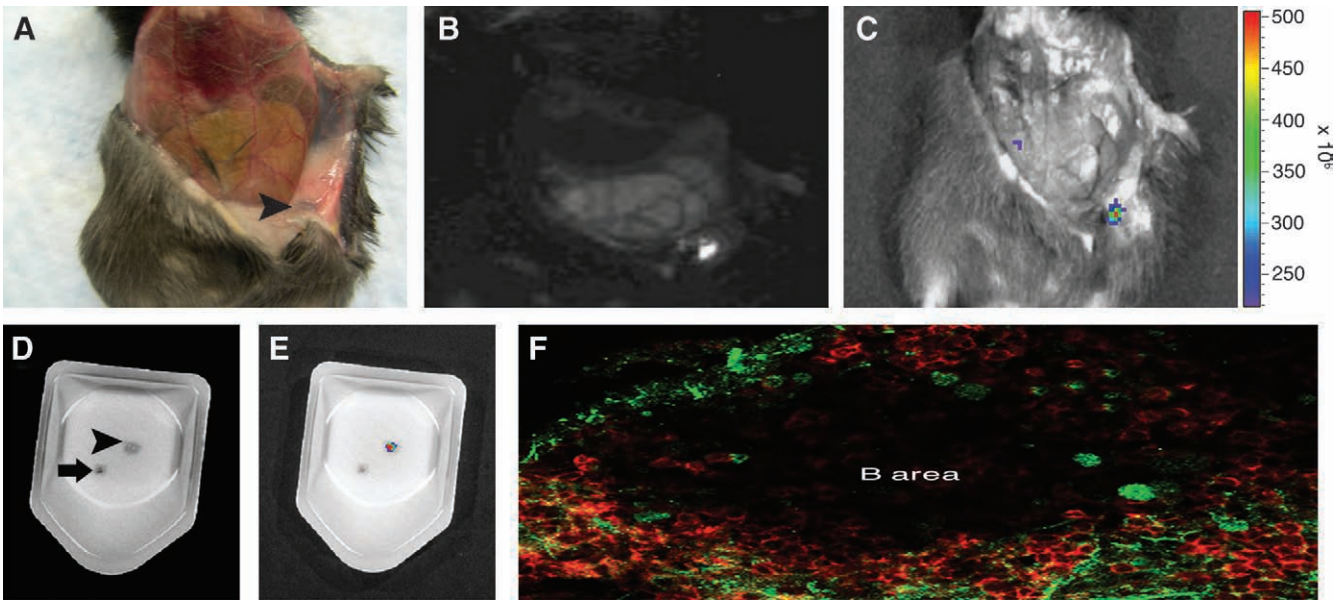


**Figure 5.** *Images of a mouse injected s.c. with DCs labeled with 6 μM $MPA_{11}$P-FITC probe. (A) Twenty-four–hour postinjection, the digital image showed the exposed inguinal LN as indicated by an arrowhead. (B) Intravital optical imaging of labeled DCs migration to the LN. (C) False-color merged image of the LN. (D) The LN was dissected for ex vivo imaging compared with the muscle; an arrow indicates the muscle. (E) Color-coded image. (F) Immunohistological analysis of a frozen section of a LN. Partial view of a LN at the follicle area: the labeled DCs (green) are associated with Rhodamine-labeled CD3 (red) indicating that the DCs are in the T-cell area. The image was taken using a confocal microscope; original magnification, ×40.*

the DCs without assisted delivery is about 18 to 24 hours [23,24]. The $MPA_{11}$P-FITC probe was internalized inside the cytoplasm; this is similar to what we observed with other cell types [17,25]. We did not observe any detectable signal when DCs were incubated with equivalent concentrations of FITC dye.

From an imaging point of view, we prefer to incubate the molecular probes in the mature stage to avoid inference with the process of antigen uptake. To this end, we decided to compare the uptake rates of immature DCs compared to their mature counterparts. Extensive FACS study showed that the former could uptake the $MPA_{11}$P-FITC probe 1.5- to 2-fold better than the latter (Figure 2). This observation may not represent every single case because the parameters may vary slightly between probes or depend on the original source of DCs. However, it provides some important principles regarding the suitable time frame for labeling DCs with minimum perturbation. We did not observe any significant changes in the phenotype or function of the DCs after the mature DCs were loaded with the probe by a brief incubation; the unlabeled and labeled cells expressed similar levels of CD11c, costimulatory molecules CD80, CD86, or CCR7 (Figure 3). The labeled cells are capable of secreting IL-12 and TNF-$\alpha$ after activation, although with slightly less effectiveness ($\sim$ 10%) compared to the unlabeled cells. Furthermore, labeling DCs with $MPA_{11}$P-FITC probe can subsequently stimulate the proliferation of $CD4^+$ T-cells (Figure 3*C*). Collectively, these results strongly suggest that we could label mature DCs with the imaging probe with minimum perturbation of cellular functionality.

The fluorescent signal depicted from the labeled cells was detected in a phantom experiment (Figure 4). There was no indication of migration to distant LNs in *in vivo* experiments. In addition, not all injected DCs could migrate to the target tissue; we observed labeled DCs trapped in the fat membrane deep below the animal's skin. Even so, a portion of the migrating DCs in the LNs could provide a strong fluorescent signal compared to peripheral tissue (Figure 5, *B*, *C*, *D*, and *E*). Most importantly, confocal microscopic studies revealed that the labeled DCs can home in the T-cells area (Figure 5*F*).

Taken together, our data suggest that it is necessary to deliver a probe inside DCs for optical imaging. With a potent delivery module, the cells can function and migrate normally. In our view, DCs are ideal targets for imaging because the labeled cells are terminally differentiated when transferred to the host system. Therefore, the imaging signal is always strong compared to imaging cells that are continuously differentiated. We believe this technique can be used to deliver tumor antigens for the processing and presentation of DCs. Finally, the delivery molecule can be modified for MRI, particularly for functionalized super paramagnetic iron oxide nanoparticles and the Gd-DOTA scaffold.

**Acknowledgements**

We thank Kenneth Rock's laboratory at the University of Massachusetts School of Medicine for training on the protocol for DCs isolation. Special thanks to Lynn Matrisian and Vito Quaranta of Vanderbilt Cancer Biology for help with the cell culture facility. We are also grateful to Wasif Khan at the Vanderbilt University School of Medicine for helpful discussion, to Carol Ann Bonner at Vanderbilt Cell Imaging Shared Resource for advice during the course of work, to Michael Yi-Wen Hwang for imaging analysis, and to Dawn Thornton for manuscript preparation.

## References

[1] Mohty M, Olive D, and Gaugler B (2002). Leukemic dendritic cells: potential for therapy and insights towards immune escape by leukemic blasts. *Leukemia* **16** (11), 2197–2204.

[2] Dermime S, Armstrong A, Hawkins RE, and Stern PL (2002). Cancer vaccines and immunotherapy. *Br Med Bull* **62**, 149–162.

[3] Lenahan C and Avigan D (2006). Dendritic cell defects in patients with cancer: mechanisms and significance. *Breast Cancer Res* **8** (1), 101.

[4] Schuler G and Steinman RM (1997). Dendritic cells as adjuvants for immune-mediated resistance to tumors. *J Exp Med* **186** (8), 1183–1187.

[5] Nieland JD, Da Silva DM, Velders MP, de Visser KE, Schiller JT, Muller M, and Kast WM (1999). Chimeric papillomavirus virus–like particles induce a murine self–antigen-specific protective and therapeutic antitumor immune response. *J Cell Biochem* **73** (2), 145–152.

[6] Specht JM, Wang G, Do MT, Lam JS, Royal RE, Reeves ME, Rosenberg SA, and Hwu P (1997). Dendritic cells retrovirally transduced with a model antigen gene are therapeutically effective against established pulmonary metastases. *J Exp Med* **186** (8), 1213–1221.

[7] Chakraborty NG, Sporn JR, Tortora AF, Kurtzman SH, Yamase H, Ergin MT, and Mukherji B (1998). Immunization with a tumor-cell-lysate–loaded autologous-antigen–presenting-cell–based vaccine in melanoma. *Cancer Immunol Immunother* **47** (1), 58–64.

[8] Hsu FJ, Benike C, Fagnoni F, Liles TM, Czerwinski D, Taidi B, Engleman EG, and Levy R (1996). Vaccination of patients with B-cell lymphoma using autologous antigen–pulsed dendritic cells. *Nat Med* **2** (1), 52–58.

[9] Nestle FO, Alijagic S, Gilliet M, Sun Y, Grabbe S, Dummer R, Burg G, and Schadendorf D (1998). Vaccination of melanoma patients with peptide- or tumor lysate–pulsed dendritic cells. *Nat Med* **4** (3), 328–332.

[10] Wen YJ, Ling M, Bailey-Wood R, and Lim SH (1998). Idiotypic protein–pulsed adherent peripheral blood mononuclear cell–derived dendritic cells prime immune system in multiple myeloma. *Clin Cancer Res* **4** (4), 957–962.

[11] Yang W, Feng J, Chang X, Fu T, Ye X, Zhang H, Li X, Wen H, Feng L, Tong C, et al. (2007). Cytotoxic effects of T cells induced by fusion protein 6B11–pulsed dendritic cells on ovarian carcinoma cells. *Gynecol Oncol* **105** (1), 238–243.

[12] Yu JS, Liu G, Ying H, Yong WH, Black KL, and Wheeler CJ (2004). Vaccination with tumor lysate–pulsed dendritic cells elicits antigen-specific, cytotoxic T-cells in patients with malignant glioma. *Cancer Res* **64** (14), 4973–4979.

[13] de Vries IJ, Lesterhuis WJ, Barentsz JO, Verdijk P, van Krieken JH, Boerman OC, Oyen WJ, Bonenkamp JJ, Boezeman JB, Adema GJ, et al. (2005). Magnetic resonance tracking of dendritic cells in melanoma patients for monitoring of cellular therapy. *Nat Biotechnol* **23** (11), 1407–1413.

[14] Shu S, Cochran AJ, Huang RR, Morton DL, and Maecker HT (2006). Immune responses in the draining lymph nodes against cancer: implications for immunotherapy. *Cancer Metastasis Rev* **25** (2), 233–242.

[15] Ahrens ET, Flores R, Xu H, and Morel PA (2005). *In vivo* imaging platform for tracking immunotherapeutic cells. *Nat Biotechnol* **23** (8), 983–987.

[16] Inaba K, Inaba M, Romani N, Aya H, Deguchi M, Ikehara S, Muramatsu S, and Steinman RM (1992). Generation of large numbers of dendritic cells from mouse bone marrow cultures supplemented with granulocyte/macrophage colony–stimulating factor. *J Exp Med* **176** (6), 1693–1702.

[17] Pham W, Kircher MF, Weissleder R, and Tung CH (2004). Enhancing membrane permeability by fatty acylation of oligoarginine peptides. *Chembiochem* **5** (8), 1148–1151.

[18] Pham W, Zhao B-Q, Lo Eng H, Medarova Z, Rosen B, and Moore A (2005). Crossing the blood–brain barrier: a potential application of myristoylated polyarginine for *in vivo* neuroimaging. *Neuroimage* **28** (1), 287–292.

[19] Austyn JM (1996). New insights into the mobilization and phagocytic activity of dendritic cells. *J Exp Med* **183** (4), 1287–1292.
[20] Steinman RM and Swanson J (1995). The endocytic activity of dendritic cells. *J Exp Med* **182** (2), 283–288.
[21] Steptoe RJ, Ritchie JM, Jones LK, and Harrison LC (2005). Autoimmune diabetes is suppressed by transfer of proinsulin-encoding Gr-1+ myeloid progenitor cells that differentiate *in vivo* into resting dendritic cells. *Diabetes* **54** (2), 434–442.
[22] Lucignani G and Rescigno M (2005). The role of molecular imaging in the development of dendritic cell–based cancer vaccines. *Eur J Nucl Med Mol Imaging* **32** (7), 725–730.
[23] Radhakrishnan S, Celis E, and Pease LR (2005). B7-DC cross-linking restores antigen uptake and augments antigen-presenting cell function by matured dendritic cells. *Proc Natl Acad Sci USA* **102** (32), 11438–11443.
[24] Woelbing F, Kostka SL, Moelle K, Belkaid Y, Sunderkoetter C, Verbeek S, Waisman A, Nigg AP, Knop J, Udey MC, et al. (2006). Uptake of *Leishmania major* by dendritic cells is mediated by Fcγ receptors and facilitates acquisition of protective immunity. *J Exp Med* **203** (1), 177–188.
[25] Medarova Z, Pham W, Farrar C, Petkova V, and Moore A (2007). *In vivo* imaging of siRNA delivery and silencing in tumors. *Nat Med* **13** (3), 372–377.